

## An introduction to molecular spintronics

JIANG ShangDa<sup>1</sup>, GOß Karin<sup>1</sup>, CERVETTI Christian<sup>1,2</sup> & BOGANI Lapo<sup>1\*</sup>

<sup>1</sup>*Physikalisches Institut, Universität Stuttgart, Pfaffenwaldring 57, 70550 Stuttgart, Germany*

<sup>2</sup>*Max Planck Institut für Festkörperforschung, Heisenbergstrasse 1, 70569 Stuttgart, Germany*

Received April 5, 2012; accepted April 8, 2012

We review the progress and future possibilities in the emerging area of molecular spintronics. We first provide an overview of the different transport regimes in which electronic nanodevices can operate, then briefly overview the important characteristics of molecular magnetic materials that can be useful for application in spintronics and we eventually present several schemes to include such systems into spintronic nanodevices. We highlight the importance of a chemical approach to the area, and in the last section we showcase some approaches to the creation of hybrids made of carbon nanostructures and molecular magnets, which are gaining increasing attention.

**carbon nanostructures, molecular spintronics, molecular magnetism, quantum transport, electronic nanodevices**

### 1 Introduction

The field of molecular spintronics is the natural combination of two fields: spintronics and molecular electronics. Spintronics studies how the magnetization state of one or more magnetic materials can influence the current that is passed through them. This field has gained enormous attention since these effects were shown to be very strong in very thin structures, and now finds application in a variety of devices, most notably in the logical and memory units of computers. Despite this extremely rapid growth and shift to applications, the field still holds a number of fundamental problems, and new physical effects are being discovered. Several excellent reviews are available to the interested reader, and here we will only sketch out the main concepts of the subject, necessary for the understanding of the present state of molecular spintronics. It should be noticed, anyway, that since at least twenty years, much of the research in this area has aimed at explaining the physical ef-

fects that arise when one or more of the components are reduced to nanosize dimensions. Even though the fabrication and characterization of such systems has mainly seen physical methods at work, the field is rapidly moving towards sizes that are comparable to that of single molecules, which will likely represent the final attainable level of miniaturization. An audience of chemists should then be aware that there is a huge research field that is just appearing on the horizon, where the chemical design of the system will largely contribute to the functionality of the devices.

On the other hand, before the study of spin effects in transport through molecules becomes feasible, one must understand the effect of transport through molecules themselves. This is the domain of molecular electronics [1, 2], which studies what happens when one part of an electric circuit is reduced in size to a single-molecule level. Three main approaches have been followed to this aim: the first is to assemble the molecules on a surface and then measure the system via a conducting tip [3, 4]; the second is to produce gaps in a metal that are only a few nm wide, where molecules can then be sandwiched [5–7]; the third is to reduce the dimensions of a conducting system, usually an

\*Corresponding authors (email: lapo.bogani@pi1.physik.uni-stuttgart.de)

organic one like carbon nanotubes (CNTs) [8, 9] or graphene [10, 11], so as to turn its density of states into a set of discrete energy levels. Whatever the approach the resulting device will contain lead electrodes, which act as reservoirs of electrons, and a quantized system in between, which is called a quantum dot (QD) [12]. Many interesting physical phenomena have been evidenced using such systems, and several excellent reviews and books on the field already exist, which treat the transport of one or more QDs depth [13–15]. Here we will thus limit ourselves to explaining the basic concepts of this area, in a way that should be accessible to chemists and material scientists alike, so as to prepare the basis for the following discussion of molecular spintronic effects. It should be understood, anyway, that the physics of these devices constitutes a very active field of research in itself, which will offer a very fertile ground when mixed with spintronics.

The key element to merge these two fields is the use of magnetic molecules, which saw a very fast development in the last three decades. The field of molecular magnetism allows creating magnetic materials whose properties can be tuned with the means of classical synthetic chemistry, for example changing the ligands surrounding a metal center or their disposition, or by tuning the molecular bridges that link two magnetic centers [16, 17]. In the last decades, chemists have developed a huge library of ligands and compounds to choose to design the magnetic properties of these systems [18]. They have also been able to relate many magnetic properties, such as the exchange interaction or the magnetic anisotropy, to structural features, and thus managed to rationalize the behavior of entire classes of compounds. It is thanks to these tools that the first molecular clusters with a high spin ground state were created, at the end of the 1980s [19, 20]. It was later discovered that such clusters can retain their magnetization for long times at low  $T$ , leading to the opening of a hysteresis cycle of dynamical origin [20]. This opened the possibility of storing information at the single-molecule level, and, on the fundamental level, allowed the study of dynamical magnetic processes on perfectly monodisperse systems, which possessed unprecedented cleanliness [21]. It was soon realized that quantum features could be observed on the magnetization dynamics of such systems [22–24], and a whole area of physical investigation developed, leading to the observation of macroscopic quantum tunneling of the magnetization [25], Berry phase interference and quantum parity effects [26, 27]. The presence of these quantum properties stimulated research also in the possible use of molecular clusters as computational units for quantum logics, and several studies now indicate that these systems could indeed constitute the basis for solid-state quantum logical systems [28].

The present review is calibrated to introduce the interested reader to the field by giving a framework where he can orient himself, whatever his background. We particularly calibrate the exposition of the concepts so that it can

be accessible to synthetic chemists and experimentalists of other fields alike. We first introduce the basic concepts of quantum transport and the different regimes that can be attained in nanodevices, and the different conceptions of the devices that lead to them. We then briefly introduce the main characteristics of molecular magnets. In the fourth section we sketch the different possible ways of attaining molecular spintronic devices and connect them to present experimental results. Eventually we concentrate on the chemistry of one of the detection schemes, which seems particularly promising for its completeness and for the chemical challenges it poses.

## 2 A brief overview of quantum transport

Electrons in bulk metals are delocalized over collective states and the overall electronic states shall be described by band theory. On the contrary, the electronic states of molecules are strongly quantized and often localized, with delocalization playing a role especially when groups and functionalities involving  $\pi$  orbitals are present. Thus, when a molecule is sandwiched between two bulk electrodes, one produces a device where two electronic reservoirs, which are characterized by partially filled energy bands, interact with a system with discrete and quantized energy levels. In the following we will discuss the fundamental mechanisms that control electron flow through such devices. It should be stated clearly, that the same situation can be produced also by sandwiching a sufficiently small piece of a standard conductor between the electrodes, i.e. creating a metallic island. It is important to state this situation clearly because this is exactly what happens when using carbon nanotubes (CNTs) for spintronic devices. If the dimensions of the metallic system are reduced to such a small size as to lead to a quantization of the electronic band structure, we can produce a quantum dot (QD), i.e. a set of discrete energy levels that resemble what is naturally found in molecules. QDs can be assimilated to “artificial molecules” and form good quasi-zero-dimensional systems, but it is important to clearly state some differences: in molecules the energy level spacing is defined by the choice of the system and can be varied using different chemical constituents and arrangements of the molecular structure; in QDs the level spacing largely depends on the material chosen and the size of the system. The typical dimensions necessary to observe quantum effects are between tens and several hundreds of nanometers, depending on the material. While quantum behaviour appears for a few atoms of a metal [29, 30], it can emerge in structures that are several nanometers large for semiconducting systems [13, 15, 31–33], while several hundreds of nanometers are sufficiently small to achieve quantization of the energy levels in CNTs [9, 34].

The electronic properties of electronic devices based on single molecules or QDs are usually investigated via transport measurements by connecting them to leads. The

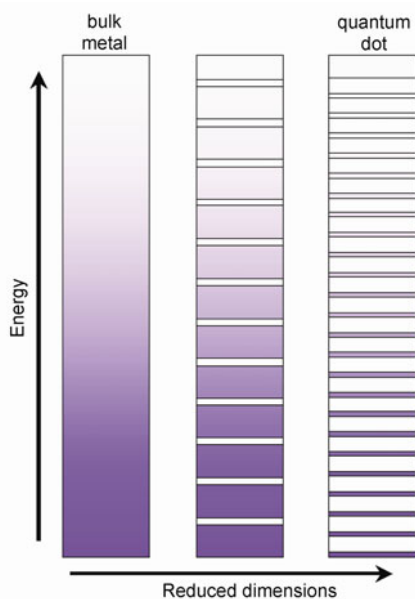


**Figure 1** Finite-size effects leading to the creation of a set of quantized energy levels from a metallic band structure when the system is reduced to nanoscopic dimensions. In the original band structure (left) a number of small energy gaps start appearing when the dimension of the system is progressively reduced, creating a number of small energy bands (center). Reducing the size of the system even further leads to the presence of only a small number of allowed occupational states, which are differently spaced based on the actual dimension of the system (right).

following discussion about quantum transport holds equally for devices with a molecule or any other kind of quantum dot. Hence, the two terms can be used interchangeably. It must be stressed, here, that a sizeable energy barrier can develop between the QD (or the molecule) and the leads themselves. At low temperatures the presence or absence of the barrier can lead to a completely different response of the molecule sandwiched between the leads. As a rule of thumb different mixings of the molecular electronic states with the delocalized wavefunction of the electrodes will cause different barrier heights, and we can distinguish three main regimes: (1) a strong-coupling regime, where the molecular states are strongly hybridized with those of the bulk metal, leading to small barriers; (2) a weak-coupling regime, where the molecular states are well separate and distinct from those of the leads, and the barriers are high; (3) a physically very rich and interesting intermediate regime, where the molecular/QD levels are only partially mixed with those of the leads, and the molecule can still retain its identity, but can be easily accessed by the lead electrons.

As the height of the barrier will generally lead to different regimes, it is thus important to understand, at least intuitively, what is its origin. For molecules the barrier height is usually varied using one of two strategies: the first approach involves changing the group responsible for the grafting onto the lead; a second approach involves inserting a non-conjugated molecular spacer, e.g. an alkyl chain, between the grafting group and the molecule itself, as schematized in Figure 2 [35].

The proof of principle of the strategies have been implemented experimentally, the first using different sulphonated ligands to SMMs to Au leads, and the second using alkyl spacers between strongly binding thiol groups and a central molecular core, constituted by a  $\text{Co}(\text{terpy})_2$  complex (Figure 2).

In addition to the source and drain electrodes, a gate electrode is usually added to the device, so as to be able to tune the electrostatic potential by a capacitive coupling. Experimentally, this is usually implemented by building the devices over doped Si wafers with a 100–300 nm  $\text{SiO}_2$  layer on top creating a backgated device [9, 36]. The same effect can also be obtained using top-gates or side-gates, as sometimes necessary when the device includes more than one QD [37–39]. The final circuit diagram representing a typical three-terminal device is sketched in Figure 3.

The behavior of the system shall then be schematized by introducing a quantity called the quantum of conductance  $G_0 = e^2/h$ , which can be used to classify the characteristics of our devices. The second range that defines the transport characteristics of our devices is the energy of the conduction channels. Two main quantities will define the behaviour of our system: the spacing of the quantized levels,  $\delta$ , discussed above and the energy  $E_C$  which needs to be spent to overcome the Coulomb repulsion when adding an electron to a system already containing some. The absolute energy scale will depend on the level of confinement of the electrons and on the system in consideration, and is usually of the order of eV for single atoms.

Once these scales are defined we can draw, following previous considerations, a rather general and basic sketch of the different regimes in which an electronic device can operate (Figure 4). Several boundaries can be defined. Let us consider the limiting situations first. If the conductance  $G$  through the device is large and  $G \gg G_0$ , a large number of

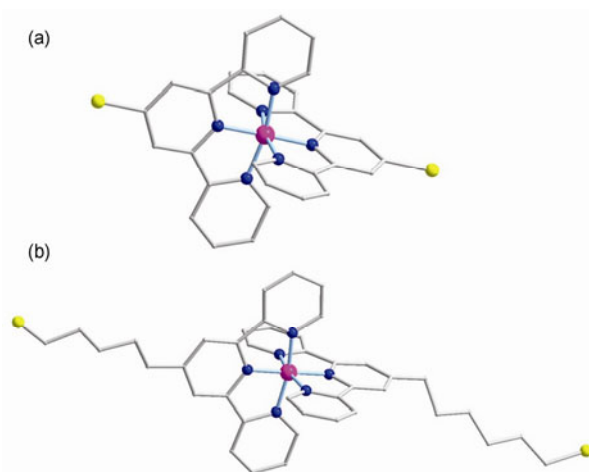


**Figure 2** Structure of molecules used to observe strong and weak couplings with the leads by introducing a five-carbon alkyl chain [35]. (a) Weak coupling.  $[\text{Co}(\text{tpy}-(\text{CH}_2)_5\text{-SH})_2]^{2+}$ ; (b) strong coupling.  $[\text{Co}(\text{tpy-SH})_2]^{2+}$ .

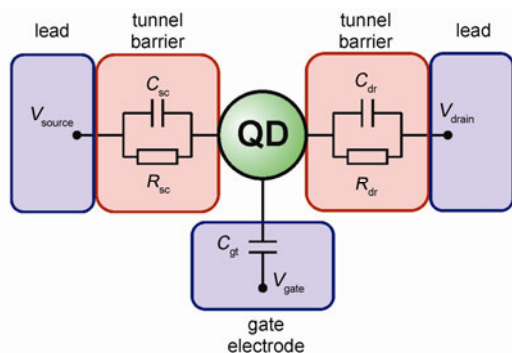


**Figure 3** Circuit diagram of a typical nanoelectronic device. The molecule or quantum dot is connected to two leads—source (sc) and drain (dr)—via tunnel barriers, each represented by a capacitance  $C_{sc/dr}$  and a tunnel resistance  $R_{sc/dr}$ . A gate electrode is capacitively coupled to the dot  $C_{gt}$ . A bias voltage can be applied via  $V_{source}$  and  $V_{drain}$  and the electrostatic potential on the dot can be tuned by  $V_{gate}$ .

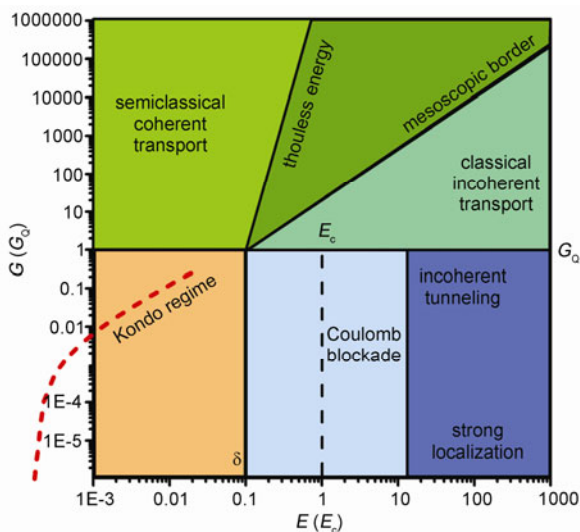


**Figure 4** Basic diagram of the regimes in which a nanoelectronic device can operate. The vertical energy scale is given in units of the quantum of conductance ( $G_0$ ), while the horizontal one, which defines the level statistics, is in terms of Coulomb charging energy ( $E_C$ ).

electrons are traveling through our device simultaneously and this will happen via a number of ways, called transport channels. If, on the contrary,  $G \ll G_0$  the electrons will get through the QD only very rarely in discrete events. The regime for which  $G \sim G_0$  is still under intense theoretical and experimental investigation and constitutes one of the boundaries of our diagram.

For  $G \gg G_0$  the electrons can spend different amounts of time on the QD, and as any time scale is related to a corresponding energy scale by the Heisenberg uncertainty principle, we can define a so-called Thouless boundary around  $2\Delta E \Delta t \sim \hbar$ . This boundary provides an upper energy limit for coherent transport with multiple channels, which is a semiclassical regime. At energies higher than this boundary we will find a region where electron-electron interactions,

which work destructively against any form of coherence, become dominant. This second boundary will be found when the time that the electron spends on the QD is approximately the same as the inelastic scattering time. Above this energy we will thus operate in a completely classical regime, while below this energy the conductors are better described as a collection of smaller nanostructures, so that the boundary region is usually called the mesoscopic border.

Once the three main regions with many transport channels are defined, we now move to devices in which there is only 1 quantum of conductance or less. The region defined by  $G \ll G_0$  and  $E \gg E_C$  is characterized by a strong localization of the electronic excitations and a conduction mechanism dominated by electron hopping, and is usually called the strong-localization regime. The most important region, for our purposes, is the one at lower energies, where the charging energy becomes the fundamental energy scale, which is called the Coulomb blockade regime of a nanodevice. When we are in this region and close to  $G_0$ , we can place the electrons one by one onto the QD during our transport measurements. This means that we will have incoherent tunneling of the electrons onto the molecule through the aforementioned energy barriers with the leads, and one can manipulate electrons one by one. The energy scale  $\sqrt{E_C \delta}$  will define a boundary between regions where this tunneling happens elastically and where inelastic tunneling effects dominate. It should be noticed that, if one can operate in the coherent tunneling region and build devices with superconducting electrodes, one can create quantum devices of almost macroscopic size. As we discussed above, the barrier energy between the QD and the leads is fundamental. When its transparency becomes high enough that the electromagnetic environment can affect the QD, we fall into the bottom-left region of the diagram. In this region the distinction between the states of the QD and the leads becomes blurred. In certain cases the electrons that pass through the magnetic QD will perceive it only as a magnetic impurity, which screens the electron flow. This regime, which is of high theoretical and experimental interest, is called the Kondo regime [35, 40, 41], and is obtained only for strong coupling of the QD to the leads.

Now that we have defined this general background, we will ignore most of the mentioned areas and we will concentrate on two of them: the Coulomb blockade regime and the region to its left – the Kondo regime.

Let us examine the Coulomb blockade first. In the three-terminal setup of a quantum dot, two voltages are available to manipulate the electronic environment of the QD/molecule: the bias voltage  $V_{bias}$ , i.e. the difference in chemical potentials of the source and the drain electrode, and the gate voltage  $V_{gate}$ . In the linear response regime, only a small bias voltage is applied and the current via the QD is measured as a function of gate voltage. In the case of

a weak coupling and sufficiently low  $T$ , generally, no state of the QD is aligned within the small bias window, as sketched in the left panel of Figure 5(a), so that the number of electrons on the dot,  $N$ , is fixed and no current is measured. Increasing  $V_{\text{gate}}$  lowers the QD potential, and when a level is aligned within the bias window, one electron can tunnel from the source onto the dot and off into the drain. In this way a non-zero current is measured only in the proximity of the QD energy levels (center panel of Figure 5(a)). Increasing  $V_{\text{gate}}$  further fills the dot with one more electron from the source, and, by sweeping the voltage we can subsequently fill the dot with electrons. The conductance measurement thus exhibits so-called Coulomb oscillations in the current across the QD, as in Figure 5(b) [42, 43].

Another way to measure transport via the quantum dot is by changing  $V_{\text{bias}}$ . Keeping  $V_{\text{gate}}$  constant and increasing  $V_{\text{bias}}$ , the changes in the number of available states in the bias window can be monitored by the differential conductance  $dI_{\text{dot}}/dV_{\text{bias}}$ . Whenever one additional dot level falls into resonance with the Fermi energy, one more transport chan-

nel opens up and the current increases observed as peaks in the differential conductance. By varying both available voltages, a conductance map can be constructed as function of  $V_{\text{gate}}$  and  $V_{\text{bias}}$ , forming the stability diagram of a quantum dot. As sketched in Figure 5(c), the diagram consists of diamond-shaped regions, called Coulomb diamonds, where the number of electrons on the dot is fixed. The diamonds are connected by ridges where the differential conductance is high, and which follow the evolution of the energy level of the QD when we are applying potentials to the leads and/or gates.

It should be stressed here that this map is a *form of spectroscopy* of the QD/molecule: in standard spectroscopy one sends photons onto the system, and measures absorption or transmission at different energies of the incoming particles. Here we can observe the excitations of one single molecule and its electronic, vibrational and spin energy levels by measuring the transmission of electrons through it. Analogously to other forms of spectroscopy, from the  $V_{\text{gate}}$  and  $V_{\text{bias}}$  one can extract the essential information of the molecule. The energy needed to add one electron to the molecule and the gate coupling parameter can be extracted from the height and the width of the Coulomb diamonds (Figure 5(b) and (c)). In general, the two slopes forming the edges of the Coulomb diamonds are not symmetric and depend on the dimensionless coupling parameters  $\alpha_i = C_i/C$  ( $i = \text{sc, dr, gt}$ ;  $C = C_{\text{sc}} + C_{\text{dr}} + C_{\text{gt}}$ ), which hence can also be extracted [13, 14]. Along the edge of the diamond with positive (negative) slope, the dot level is aligned with the Fermi level of the source (drain) and such regions are called source (drain) resonances. The transitions involving vibrational or spin excited states of the single-particle energy spectrum are found as resonance lines running parallel to the diamond edges. The energy-level spacing can be extracted from the bias window at the meeting point of an excited state resonance line with a diamond edge. Following these lines as a function of some other external parameters (like magnetic field, etc...) allows observing spin or other effects that affect the QD. For example a splitting of a resonance line associated with spin excitations is usually expected when applying a magnetic field, and can provide information on the spin system under investigation. In summary, it is possible to fully characterize a QD/molecule from its stability diagram. The capacitances which couple the dot to the environment can be determined, as well as the quantum level structure and the excited state spectrum including spin excitations. In this sense, quantum transport serves as a spectroscopic method, capable of detecting single molecules and their properties.

The second regime which we are concerned about is the one in which the transparency of the barriers becomes very high. One can picture this situation as similar to the case in which one atom (which has a quantized energy spectrum when alone) is bound to a bulk metal, which has a continuum of states defined by its band structure. Until now we

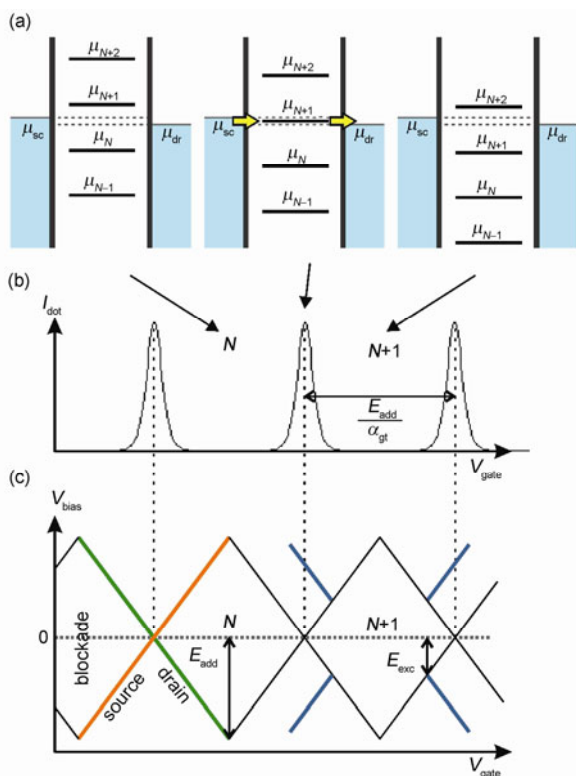


**Figure 5** (a) Schematic of the quantized states of the electrochemical potential of a quantum dot for three different level alignments. The gate voltage increases from left to right. If there is no dot chemical potential aligned within the bias window, the number of electrons on the dot is fixed ( $N$ ) and it is in Coulomb blockade. No current can be measured. Increasing  $V_{\text{gate}}$  lowers the dot chemical potentials and when one of the levels is aligned within the Fermi energy of the leads, electrons tunnel across the dot and a non-zero current  $I_{\text{dot}}$  is measured; (b) Coulomb oscillations in the current  $I_{\text{dot}}$  across the QD; (c) schematic differential conductance  $dI_{\text{dot}}/dV_{\text{bias}}$  plot exhibiting Coulomb diamonds and excited state resonances. The addition energy  $E_{\text{add}}$  and the energy  $E_{\text{exc}}$  of an excited state are indicated.

have considered the situation when the interaction is not so strong (e.g. when depositing n-heptane on Au). Then, the energy levels of the molecule remain well-defined, in a situation similar to our case of high energy barriers. On the other hand it is clear that, if their bonding is good (e.g. adding a Co atom to an Au surface), the atom will then become part of the metal and the individuality of its energy states will be lost, which is equivalent to saying that the barrier is low, in our case. This second situation is usually schematized using the Kondo regime for QDs, where co-tunneling effects are possible. That means, that an electron may tunnel onto the QD while another electron tunnels off, as sketched in Figure 6(a) and (b). In this case, the electronic states of the QD/molecule become strongly hybridized with those of the leads and a quasi-continuum of states will develop. This many-body state leads to a peak in the density of states at the Fermi level (Figure 6(c)), which will be detected as a characteristic peak of conduction at zero bias voltage, often called a “Kondo ridge” (Figure 6(d)). Following the initial assumption made by Kondo to explain the resistivity of metals with magnetic impurities at low  $T$ , one starts considering that the spin  $S$  associated with the QD is coupled with the electrons on the conduction band,  $S$  and the spins of the conduction electrons have to align antiparallel to minimize the total energy. This leads to a screening of the electrons flowing through the device by the spin  $S$  when there is an odd number of electrons on the QD, while an even number of electrons usually produces no effect.

### 3 Molecular magnetic materials

Molecular magnetism is the research area that is concerned with designing, synthesizing and investigating molecular materials with magnetic properties. As such it is already a

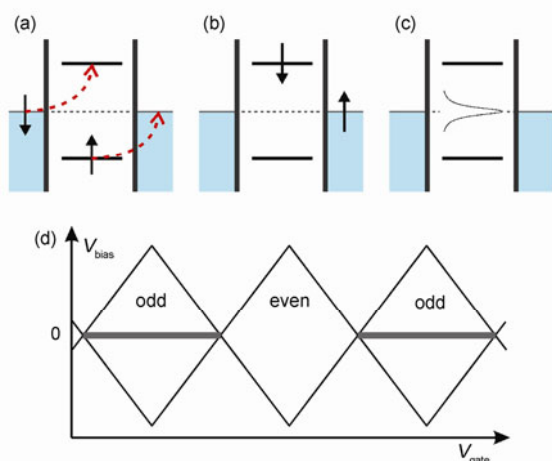


**Figure 6** Schematic of the Kondo effect. (a, b) A co-tunneling process changing the spin on the QD; (c) a finite density of states at the Fermi level arises; (d) a non-zero conductance (Kondo ridge) is observed in the Coulomb diamonds corresponding to an odd number of electrons on the QD.

rather wide area, but, over the years, it has expanded even further to include magnetic materials obtained by molecular approaches. For many years the field mainly concentrated on obtaining organic ferromagnets from extended networks, following the idea that, since organic frameworks can show metal-like conducting properties (see also below), there should exist the possibility of creating organic ferromagnets. Room temperature organic ferromagnets have turned out being much more difficult to obtain than organic conductors and semiconductors, so that this task remains unachieved. One of the main reasons of this failure is that the use of organic ligands actually promotes the formation of low-dimensional materials, such as clusters and chains. Realizing this limit has led to one of the most fertile areas of research of the last three decades giving rise to a fertile interdisciplinary field between physics and chemistry. The peculiarities of molecular structures have allowed monitoring the interplay of classical and quantum effects in magnetism, and observe several quantum features like quantum tunneling of the magnetization and Berry phase interference. This allows creating spintronic devices where the magnetic part behaves quantum mechanically, in contrast to present devices where the magnetic part has classical behaviour. In this paragraph we will not provide an in depth coverage of all the aspects of the field, and we will try to collect, according to the authors' sensitivity, the main results for which molecular magnets have a particular added value for molecular spintronics. Books or authoritative reviews covering the different aspects of molecular nanomagnets are available, and we address the interested reader to them at the relevant points [17, 18, 44, 45].

Synthesizing molecular clusters made of several magnetic centres is relatively easy and there already exists a huge library of metal ions and organic radicals that can be used to this aim. When creating chain systems or metal clusters the molecular nature works to our advantage, rather than against us, as happening when creating three-dimensional magnetic networks. The bottom-up approach typical of molecular chemistry allows building the magnetic molecules almost ion by ion and, at the time of the writing of this review, larger and larger clusters continuously appear, some of which already reach the size of magnetic nanoparticles.

The field of single molecule magnets (SMMs) has basically been started by the observation of unusual magnetic properties in clusters comprising twelve manganese(III, IV) ions,  $Mn_{12}O_{12}(O_2CR)_{16}(H_2O)_4(Mn_{12})$  [46, 47]. The acetate derivative ( $R=Me$ ) was first prepared by Lis, while the benzoate derivative ( $R=Ph$ ) was studied by Christou and Hendrickson [19], during a systematic investigation of Mn-based clusters as models of photosystem II. The breakthrough came with the sound interpretation of the magnetic properties of  $Mn_{12}Ac$  [20, 48] and the observation of a hysteresis of molecular origin [21]. The second breakthrough, which could be established only due to the molecular nature of the compounds, was the discovery that the

relaxation of the magnetization of Mn12 clusters occurs via thermal activation plus a tunnel mechanism [23, 24]. This discovery and the accessibility to the related quantum effects opened the field to a much broader audience and provided a common ground for physicists and chemists in the field.

The majority of efforts in the synthesis of SMMs are currently devoted to: (1) increasing the size of the clusters; (2) increasing the spin in the ground state  $S$ ; (3) increasing the temperature below which hysteresis is observed (a.k.a. blocking temperature, or  $T_B$ ); (4) arranging and organizing SMMs on surfaces or into hybrid structures. As a result of this research, clusters approaching the size of small proteins have been created, like the beautiful torus-shaped  $Mn_{84}$  cluster with a diameter of 4.2 nm, and an inner hole of 1.9 nm [49]. The ground spin state has been increased up to  $S = 83/2$  (in a Mn19 complex) [50] and a  $T_B$  up to 8 K has recently been obtained in U-based compounds [51], i.e. about 5 K above the longstanding  $T_B$  record of  $Mn_{12}$  clusters.

Although SMMs have been known for almost 30 years, more and more insight is continuously obtained. Most of the work on SMMs concentrates on the low- $T$  behaviour, which is usually interpreted using the “giant spin (GS) approximation”, i.e. assuming a defined spin value  $S$  in the ground state (for example  $S = 10$  in  $Mn_{12}$  complexes). The degeneracy of this manifold is lifted by the presence of a magnetic anisotropy. When including the application of a magnetic field (Zeeman effect) the low- $T$  spin Hamiltonian reads:

$$H = DS_z^2 + E(S_x^2 - S_y^2) + \mu_B SgH + \sum_{n=2 \dots 2S} \sum_{k=1 \dots n} B_n^k O_n^k \quad (1)$$

where the first two terms describe the first-order molecular anisotropy, the third is the Zeeman splitting due to the magnetic field and the last term is a multipolar expansion of crystal field effects using the Steven's operators [52]. The symmetry of the system will determine which  $B_n^k$  coefficients are nonzero: when the symmetry is tetragonal, as in some  $Mn_{12}$  complexes, only terms with  $k = 0, \pm 4$  are to be included. These crystal field terms provide information on the magnetic anisotropy and consequently on the magnetic relaxation. Transverse anisotropy terms (i.e. those with  $k \neq 0$ ) are particularly relevant, since they influence the tunnel frequency. It is important to stress that the parameters can be extracted from high-field electron paramagnetic resonance (EPR) measurements and then compared to the magnetic behaviour of the systems. This is usually performed by taking into account the slow relaxing behaviour of SMMs, which we briefly describe below.

The presence of a  $D < 0$  anisotropy parameter leads to the presence of an axial magnetic anisotropy of the system, i.e. the magnetization will preferentially lie along one axis of the SMM, while it will require increasing energies to move it further and further away from this axis. This is schematized in the double-well potential diagram reported

in Figure 7. Once the SMM becomes trapped into one of the wells, e.g. after application of a magnetic field, it can only escape by overcoming the energy barrier via thermal activation or by tunneling through the barrier via a quantum mechanical process. The former mechanism will become very improbable at sufficiently low temperatures, while the latter will remain an available channel whatever the temperature.

Several examples show striking agreement between the energy diagrams calculated with the EPR parameters and the pattern of magnetic relaxation observed, with an almost perfect match between the fields for which the avoided level crossings are calculated and the experimental ones (see Figure 8). Such extremely accurate predictions allow testing a good deal of quantum physics, and several prominent examples have appeared such as the testing of Kramer's parity theorem and the observation of Berry phase interference.

From the point of view of molecular spintronics these properties are interesting because they allow inserting a magnetic system with quantum properties into spintronic devices. Until now spintronic devices have made large use

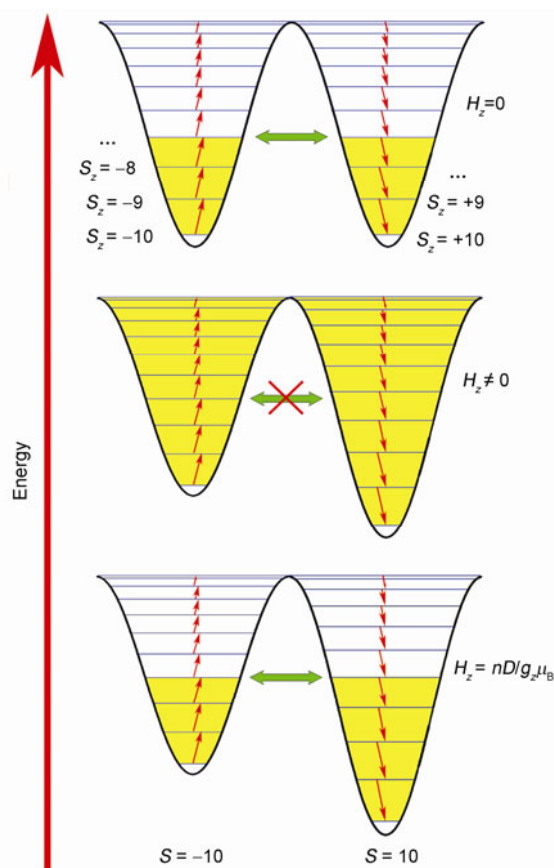


**Figure 7** Double well potential of a SMM, the typical scheme of a Mn12 SMM is used for convenience. The vertical axis represents the energy, while the  $S_z$  spin levels of the ground state multiplet are depicted within the two wells created by the axial anisotropy  $D$ . The situation for different fields is depicted, starting from zero field (top), then moving to a moderate field at which no levels are in resonance (middle) and eventually to a field where one or more levels are in resonance again (bottom).

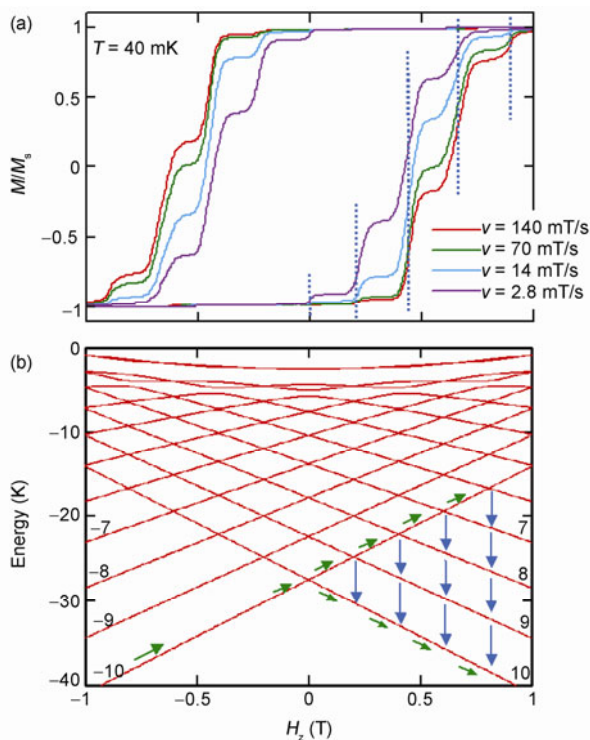


**Figure 8** (a) Experimental hysteresis loop of the Fe8 SMM, acquired at 40 mK and with different cycles corresponding to different sweeping rates of the magnetic field, as in the colorscale; (b) energy level diagram of the spin levels of the Fe8 SMM as a function of the external magnetic field, as calculated using the anisotropy parameters extracted from EPR data. The correspondence between the avoided level crossings and the observed steps in the magnetization is highlighted with the blue lines.

of quantum effects in the electronic part and the use of tunneling effects has been particularly prominent; on the other hand their magnetic components have always been constituted by large classical systems, where the magnetization reversal can be described using domain wall motion or alternative classical models. It should then be clear that SMMs offer an exceptional opportunity to produce spintronic devices with quantum properties due to the magnetic components. The main challenge is then to produce molecular magnetic systems that can be integrated into functional devices and still display the desired properties. In the following we briefly resume several strategies that have appeared along this direction.

#### 4 Magnetic molecules for quantum transport

While in the previous sections we examined quantum transport and SMMs in general, in this section we discuss several possible ways of implementing it with molecular magnetic materials. Several detection and transport schemes have been envisaged over the time (Figure 9). The most basic one is the immobilization of molecules onto a conducting surface, so as to probe the energy levels on the sys-

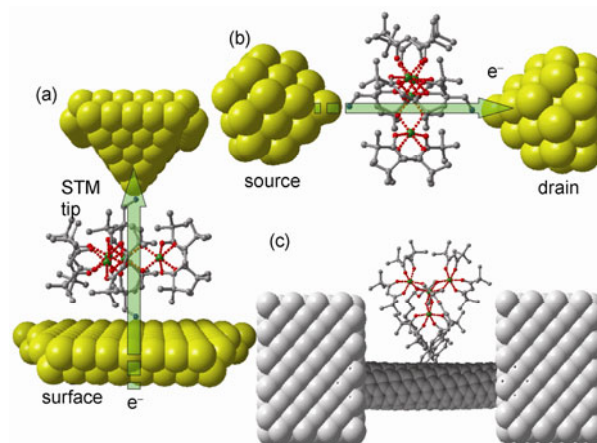


**Figure 9** Three main detection schemes in molecular spintronics. All schemes are shown as implemented with Fe4 molecular magnetic clusters. (a) Detection scheme using a conducting tip, as in a scanning tunneling microscope; (b) molecular junction device, to which a third terminal can be added by building the device on a Si wafer; (c) double magnetic QD scheme. The molecule (i.e. a spin QD) is attached onto a second, electronic QD (in this case a carbon nanotube). The effect of the molecular spin onto the current flowing into the QD is then felt and detected, leading to single molecule detection without flowing electrons directly through the spin system, and thus avoiding strong perturbations. Again a backgate electrode can be added by building the device on a Si wafer.

tem using a conducting tip, as in a scanning tunneling microscope (Figure 9(a)). The second, more advanced and more challenging approach (Figure 9(b)), is to immobilize a molecule between two electrodes and then measure the current through it, similarly to the scheme in Figure 3. The third approach consists in attaching the magnetic molecule onto a pre-existing quantum dot, so as to constitute a “spintronic double quantum dot” where the molecule acts as a spin QD and the transport occurs through a solely electronic QD coupled to the spin one (Figure 9(c)). In the following we will provide a more detailed overview of these three situations, and explain their respective advantages and disadvantages.

The first approach (Figure 9(a)) has the advantage of being more easily implementable than the other two, as it only needs the deposition of molecules on the metal surface. This has been achieved via a number of different functionalizations of SMM clusters to bind on gold and other metals. The scope of the different strategies involved and their degree of success has constituted a particular subfield of molecular magnetism for a while and the interested reader is redirected to a few very complete and detailed reviews of these efforts for reference. It should be stressed, however, that two main methods have been mainly followed: one relies on binding the molecular materials onto the surface with suitable chemical groups, like thiols for gold, while the second one relies on the immobilization of the molecules via evaporation and/or direct drop casting methods. In all cases, the effect of the substrate on the molecular magnetic properties remains unknown, even though the first steps towards un-



derstanding the interaction of the molecule with the metal substrate have already been taken. Recent experiments on depositing single  $Mn_{12}$  clusters ( $R=CH_3$ ) using advanced electrospray ion beam deposition techniques have evidenced the preservation of the single molecule properties when a thin insulating layer is sandwiched between the SMMs and the metal surface [53]. The experiments, performed in the Coulomb regime, show that, on the contrary, the transport characteristics are strongly altered when a direct deposition onto the metal is performed, a first indication of the importance of the deposition substrate. The second class of molecular magnetic materials that has been investigated is that of double-decker rare-earth complexes, which have been deposited onto Au(111) surfaces. In this case it has been possible to investigate the systems in the Kondo regime, and the presence of unpaired electrons on the  $\pi$ -orbitals of the phthalocyaninate ligand seems to contribute decisively to this regime.

The main disadvantage of this approach is the fact that one can investigate the properties of the molecules as a function of the surface-tip voltage but no external voltage source can be applied, i.e. no gate voltage is present. This is a major disadvantage because it basically restricts the investigation onto one line of the Coulomb diagram (as mentioned in section 2) and prevents a complete spectroscopic characterization of the system. Such limitations are overcome by the second type of measurements, albeit at some price.

The second type of experiments (Figure 9(b)) implies the immobilization of an intact molecule inside a nanometer-sized gap between two electrodes. Such experiments have in fact been the first to be attempted, because they offer the possibility of fully characterizing the system, even though the devices are more challenging to produce. They have the important drawback that, in contrast to STM imaging, only one molecule can be investigated and this particular molecule cannot be investigated with other means and will be imprisoned in one unique, random orientation with respect to the leads and the current flow. The experiments thus suffer from a lack of reproducibility and it is also difficult to state clearly what is in fact being probed, in absence of clear magnetic fingerprints. The most used junctions are electromigrated or break-junction devices [5], which can integrate a backgate electrode, usually buried below the junction itself. As usual, two experimental regimes can be distinguished, depending on the strength of the coupling to the electrodes: a weak coupling (or Coulomb) limit and a strong coupling limit, where Kondo effects can be probed.

The experimental realization of the weak-coupling limit has been achieved using a  $Mn_{12}$  derivative functionalized with thiol groups, which provides strong and reliable covalent bonds to the electrodes [54], which anyway create relatively high tunnel barriers. As the Coulomb blockade involves the sequential charging of the SMM, the magnetic

properties of the negatively- and positively-charged species must be considered, in addition to those of the ground state. This introduces an important difference with respect to standard molecular electronics, where charging of the molecule usually does not significantly alter the interesting degrees of freedom [55]. Positively charged  $Mn_{12}$  clusters have a lower  $D$  anisotropy [56] and the presence of these charged states is fundamental to explain the electronic transport and in particular the observed negative  $G$  values [29, 30]. Studies as a function of applied magnetic field  $H$  have shown a first evidence of the spin transistor properties [30] as well as the lack of a hysteretic response, which can be due to the breaking of the SMMs during the grafting, to the population of excited states or might also be a consequence of the interaction with the metallic electrodes, similarly to the observed interaction with conducting surfaces in the STM experiments. Further investigations have also shown that the magnetic anisotropy can be tuned using a magnetic field and that the magnetic field evolution of excited states in the stability diagram indicates a zero-field splitting [54, 57–59].

Theoretical investigations in the weak-coupling regime indicate that it should be possible to connect structural and magnetic parameters to the transport features, something that cannot be attempted with nanoparticles or QDs, as only SMMs offer perfectly identical, monodisperse and reproducible systems. Theoretical analysis shows that even films of SMMs should retain the salient properties of single-molecule devices [60, 61] and a further analysis has extended to chemically-related SMMs [62], opening the way to the use of the unique chemical potential of SMMs in testing theories with several related compounds.

The strong electronic coupling has been attained using paramagnetic molecules containing one [35] or two magnetic centers [63], but remains unachieved for SMMs. The mononuclear paramagnetic molecule investigated in this regime (Figure 2(b)) [41] shows a Kondo peak when the thiol is directly connected to the TerPy ligand, while the system with the longer alkyl spacer (Figure 2(a)) displays low transparency barriers and Coulomb blockade. Characterization as a function of  $H$  reveals the presence of spin excitations, and agree with the effective  $S = 1/2$  state attributed to  $Co^{2+}$  ions at low  $T$ . On the other hand, a Landé factor  $g = 2.1$  is found, which is unexpected for  $Co^{2+}$  ions, characterized by high spin-orbit coupling and magnetic anisotropy, and this point needs further investigation.

The possibilities offered by a simple dimeric molecule, i.e. containing two magnetic centers, have also been investigated [42] using the divanadium molecule  $[(N,N',N''\text{-trimethyl-1,4,7-triazacyclononane})_2V_2(CN)_4(\mu-C_4N_4)]$  [64]. This is again directly grafted to the electrodes, and produces very high transparencies [42]. Via the gate voltage one can tune the molecule into different charged states: a neutral state with  $S = 0$  and a positively charged state with  $S = 1/2$ . The Kondo resonance is found, as expected [37–40], only

for the state in which the molecule has a nonzero spin moment and the electron flow can be screened by the magnetic impurity. This nicely demonstrates that magnetic molecules with multiple centers and antiferromagnetic interactions permit to switch the Kondo effect on and off, depending on their charge state. The temperatures at which Kondo features are found in such systems are much higher than those obtained for QDs and carbon nanotubes [37–40]. In order to observe the Kondo regime one should orient himself to using small SMMs [21] with high delocalization, so that core states can be more affected by the lead wavefunctions.

Theoretical investigations [65, 45, 46] suggest that the Kondo effect should be visible in SMMs even for  $S > 1/2$  [66], and that the presence of even a small transverse anisotropy can produce a Kondo peak [45]. These works also show that, in addition to a sound selection of the ligands, a rational choice of the physical parameters of the spinHamiltonian is also necessary to observe Kondo behaviour in SMMs. The aforementioned Berry-phase interference [8, 23] can eventually produce a series of Kondo peaks on varying the external magnetic field [67]. These predictions show how SMMs, being molecules and having a well-determined spin Hamiltonian, can have substantially different behaviour than QDs and nanoparticles and should permit the observation of different physical phenomena.

While this detection scheme presents several advantages over the first one, it still suffers from several drawbacks, the most important of which is probably the fact that the electron flow can directly pass through the molecule, thus strongly perturbing the spin state. Such drawbacks can be further overcome by using the third detection scheme, discussed below.

The third detection scheme, which is growing in interest and relevance, consists of using a multi-dot device in a three terminal scheme, where the current passes through a non-magnetic QD only weakly coupled to the SMM. Several ways in which the spin can influence the transport properties of the conducting QD can be envisaged (Figure 10): the first is by simple dipolar coupling between the SMM magnetic dipole and the flowing electrons, and does not require any particular form of chemistry, as non-covalent grafting should be sufficient; the second is the magneto-Coulomb effect [68], already observed for magnetic nanoparticles [69] and possibly responsible of the recent observations also with SMMs [70]; the third possibility, i.e. direct exchange coupling between the SMM and the electrons [11, 54], requires a covalent functionalization of the QD, which has not been achieved yet (see the following paragraph); the fourth option is to use the QD as a detector of the magnetic flux variation, e.g. in the case of the recent nanoSQUID [70, 71]. Recently the double QD scheme has been implemented using Tb double-deckers grafted onto a CNT contacted by non-magnetic electrodes [72]. In this setup, the CNT forms a non-magnetic quantum dot, while the switching of the magnetic moment of the Tb-bis (phthalocyanine) molecules causes changes in the electronic transport depending on the applied magnetic field. The magnetic moment of the highly anisotropic lanthanide leads to a magnetic field dependence of the electrical transport, and the magnetoresistance ratio is determined as high as 300% at temperatures lower than 1 K. The same SMMs have also been coupled to a quantum dot structured in graphene [73]. In these devices, a magnetoconductivity signal up to 20% is found when sweeping the magnetic field. It should be noticed, anyway, that in both cases the exact mechanism leading to the observation of the signal remains unknown and the underlying physics shall likely become the subject of future investigation. Spin valve-like mechanisms have been proposed, but they remain to be confirmed using the tools that normally identify such behaviours, e.g. Hanle precession.

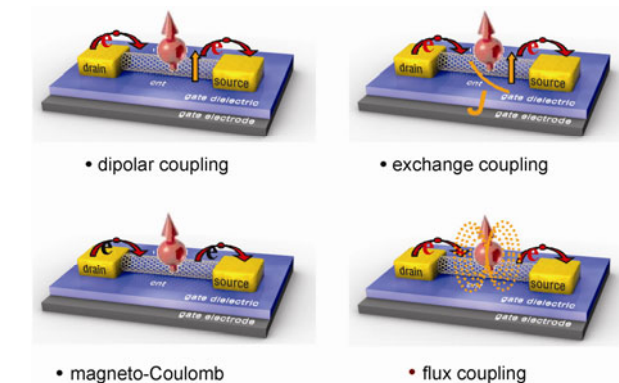


**Figure 10** Different coupling schemes between a QD (here represented as a CNT) and a SMM that can lead to the observation of spin effects on the electron flow of the CNT (red).

Eventually we wish to mention that coupling to the vibrational degrees of freedom is also possible. It has been demonstrated that carbon nanotubes (CNTs) can produce excellent resonators with extremely high quality factors. It can thus be envisaged to couple the magnetic moment to these vibrational degrees of freedom, which, in turn, can be monitored electrically [74]. Theoretical investigation already shows that single molecule sensitivity should be reachable [75].

Eventually we wish to mention that coupling to the vibrational degrees of freedom is also possible. It has been demonstrated that carbon nanotubes (CNTs) can produce excellent resonators with extremely high quality factors. It can thus be envisaged to couple the magnetic moment to these vibrational degrees of freedom, which, in turn, can be monitored electrically [74]. Theoretical investigation already shows that single molecule sensitivity should be reachable [75].

## 5 Hybrids of organic materials and magnetic molecules for quantum transport

In this section, due to the growing relevance of the third detection method, we quickly review the possibilities in the chemistry of carbon nanomaterials and molecular nanomagnets. The bulk of the work has been performed on carbon nanotubes (CNTs) [76], while some recent works point in the direction of graphene-based hybrids and devices, which can exploit the presence of Dirac electrons in the graphene structures.

The chemistry of CNTs has been well developed since their discovery and leads to some fundamental advances in functionalization and chemical manipulation [77–84]. It is worth reviewing these modification methods to develop suitable means for the functionalization of CNT and graphene with molecular magnets. Basically, the chemistry of CNTs often revolves around introducing defects on the sidewall of the CNTs to perform further reaction with target molecules. However, the defects on a CNT constitute scattering sites that severely limit the performance of electronic devices. Therefore it is of fundamental importance to reduce the defects of a CNT to a minimum level during the development of CNT-molecular magnets hybrid electronics devices.

Lots of interesting results have been reported on the creation of CNT devices [8, 70, 77–82, 85–94], however, very limited results are available on the CNT-molecular magnets hybrid devices and it is a great challenge to investigate the parameters that govern the behavior of these devices [95]. The symbol behavior of molecular based superparamagnets can be taken as evidence that the interaction between the two systems, molecular magnets and CNT, is obtained.

Single-molecule magnets (SMMs) possess the magnetically bistable states due to the Ising type anisotropy, which enable one to investigate the interaction between Ising type anisotropy and transport [95]. However, due to the partial energy transfer from the SMM to the device, it is then effective to employ systems releasing a maximum energy when reversing the magnetization. Practically, as the energy is proportional to the area of hysteresis cycle, attention should then be focused on those SMMs affording higher magnetization saturation values at a given temperature and magnetic field sweeping rate. Normally, simple paramagnetic materials can be of little interest due to the absence of magnetic behavior fingerprints on the electron flow as well as the very poor energy transfer [95].

In addition to SMMs, a second class of molecules can be those which undergo structural or electronic changes under an external stimulates, such as light for instance [96–99]. The effect of irradiation on the transport can also be taken as the fingerprints of the molecule and it can be a way to affect the functionality of the device. Lanthanides containing molecules are of great interest as well, which are able to show parity effects on magnetic properties and thus can be identified [95, 100–103].

Basically, there are two strategies to develop hybrid devices with different outcomes on the electronic properties: non-covalent [104, 105] and covalent [106, 107] binding to CNT or graphene. For the non-covalent binding to CNTs, the grafted molecule will locally alter the electron density of the CNT and thus generate a scattering center [108]. It can also be expected that the interaction between the CNT and the molecular magnet is very weak and this strategy is a good way to develop a weak coupling hybrid. The weak coupling hybrid electronic devices, if operated with suffi-

cient sensitivity, can detect the presence of one or several grafted molecules even at room temperature. It is very important to use stable molecules so as to avoid a loose of molecules from the grafting ligand attached to the CNT, which will generate unnecessary scattering centers.

Two ways are usually employed to modify the molecular magnets in order to graft them on CNTs with a non-covalent binding. The first one is to modify the ligand with tails containing polycyclic aromatic groups, like pyrene. These aromatic groups are able to form relatively strong  $\pi$ - $\pi$  stacking with a CNT, and have been used to attach nanoparticles to CNTs in solution. A method to determine the distribution of those molecules on CNTs was also developed [109, 110]. The modified molecules are assumed to stick onto the CNT randomly. Then, the probability of having two molecules at a distance  $L$  is  $P(C, L) = Ce^{-LC}$ , where  $C$  is the linear concentration of the molecules on the CNT [111, 112]. Statistical analysis of the distribution of  $L$ , performed on CNTs, revealed good agreement with the predicted law and allowed  $C$  to be extracted for each repetition. The results show that  $C$  varies linearly with the repetition times. In this way, one is able to determine the linear concentration of grafted molecules on CNTs, and thus to optimize the experimental conditions before proceeding to electronic devices.

Recently, a hybrid device with pyrene as the non-covalent binding point has been reported [113]. A double-decker molecule with a lanthanide ion sandwiched is modified with pyrene. The high-resolution transmission electron microscopy, emission spectroscopy and atomic force spectroscopy results reveal that the modified complex has been successfully attached to the CNT using  $\pi$ - $\pi$  stacking interactions. Additionally, due to the reducing intermolecular interaction, the anisotropy energy barrier and the magnetic relaxation time of the hybrid are both increased in comparison with the modified complex.

Another way to modify the molecular magnets is by addition of long alkyl chains [104, 105]. Such groups can form van der Waals interactions with the hydrophobic wall of a CNT, either with the chains lying along the CNT axis or by wrapping around its diameter. In both cases, the interactions are likely lower than in the previous case, and can certainly lower the perturbations in the electronic structure of the CNT. These ligands are thus indicated for a weak coupling between the molecular magnets and CNTs. We have coated the  $\text{CoFe}_2\text{O}_4$  nanoparticles with both pyrene and long alkyl group containing ligands and thus obtained both the aforementioned two types of modified nanoparticles [110]. However, the results reveal that a modification with the pyrene containing group yields a controlled and selective grafting, with only several nanoparticles sticking on the CNTs.

A third way to graft molecular magnets onto CNTs is to employ those SMMs with aromatic rings in the outer shell of the molecule. Without the long modification carbon

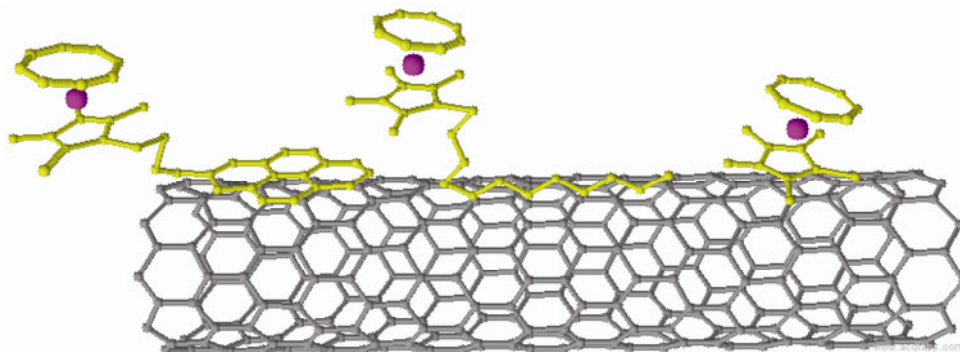


**Figure 11** Strategies to graft molecular magnets onto a CNT using non-covalent binding. (a) Modifying the ligands with tails containing polycyclic aromatic groups, i.e. pyrene, can attach the molecules via  $\pi$ - $\pi$  stacking onto a CNT; (b) another way to modify the molecular magnets is by adding long alkyl chains to form van der Waals interactions with the hydrophobic wall of a CNT; (c) employing the molecular magnets with aromatic rings out shell can generate a comparable stronger interaction between the target molecule and the CNT.

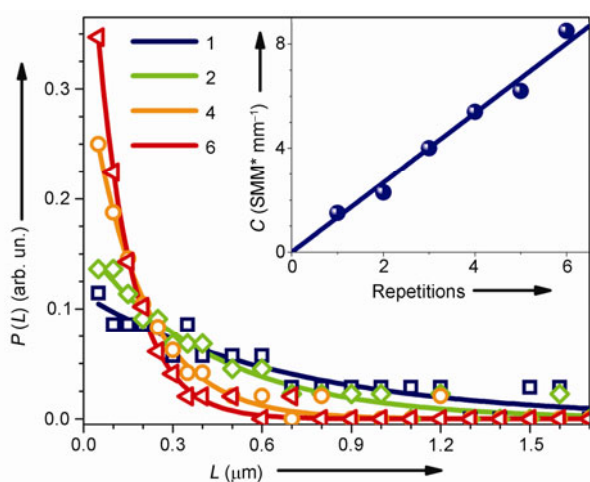


**Figure 12** Probability of finding a distance  $L$  between SMMs grafted on CNTs for sequential repetitions of the process. Symbols are experimental data for 1, 2, 4 and 6 repetition and lines are the corresponding fits. Inset: extracted linear concentration as a function of the number of repetitions of the process and linear fit.

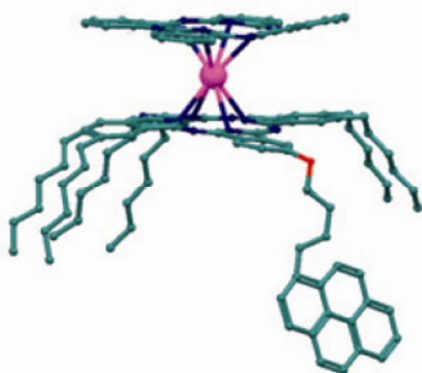


**Figure 13** The structure of the double-decker molecule with a terbium ion sandwiched in the center. One of the deckers is modified with pyrenyl and hexyl substitutions which is able to maximize the interaction with CNTs.

chains of the previous two cases, but by contacting the complex directly with the CNTs, the interaction of the mol-

ecules with the CNT can be relatively strong in comparison to the aforementioned two approaches. The grafting of a single lanthanide ion containing molecule onto CNTs has been reported via a wet adsorption method [114].

The strategy of a covalent binding to CNTs is based on the presence of occurring defects inside the CNTs [106, 107]. In the previous section we assumed that the CNT walls are formed by a perfect honeycomb lattice, however, no present synthetic method is able to yield perfect CNTs without any defects. The defective sites perform different chemical properties and thus can form a covalent bond with modified SMMs resulting in a covalent binding hybrid device. Making use of the existing defective sites, rather than non-covalent grafting, implies the advantage of avoiding the addition of more scattering centers to the already present ones. It is obvious that the covalent grafting yields a much stronger coupling between the molecular magnets and the CNTs. The investigation of how different chemical groups transmit spin interactions is becoming more necessary and the chemistry of molecular magnets can be an invaluable tool to this aim [95].

The defects are partly constituted by dislocations or changes in diameter, or by missing carbon atoms inside the CNT walls. The defective sites usually result from the severing of locally more liable carbon bonds. Alternatively, pentagon-heptagon pairs (AKA Stone-Wales defects) and vacancies can constitute reactive sites on the CNT walls. Treatment with inorganic acids, often performed in order to eliminate the catalyst used in the fabrication, can also cause a large amount of defects and should be considered with care [115, 116]. Even non-chemical treatments, such as ultra-sonication, electron beam imaging and AFM microscopy can damage the CNTs and introduce defects as well [116].

Defective sites can be divided into three types: (i) sites of  $sp^3$  hybridization with hydrogen or hydroxide groups inserted into the defective site, and oxidative defective sites with carbon atoms replaced by carboxylic groups on (ii) sidewalls or (iii) terminal sites. Normally, terminal groups cannot be exploited for molecular spintronic devices for its

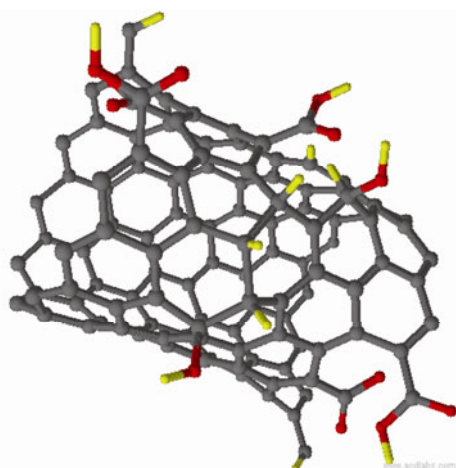


**Figure 14** Defects on a single walled CNT exploitable for the grafting of molecular magnets. Oxygen atoms are depicted in red. Three types of defects are represented: sites maintaining  $sp^3$  hybridization with  $-H$  and  $-OH$  groups were inserted into the defective site, oxidative defective sites with carbons replaced by  $-COOH$  groups on sidewalls and terminal sites, normally terminating in carboxyl groups.

difficulty in creation a two-lead device. Defects of  $sp^3$  hybridization can be difficult to exploit, because their chemistry has only been explored to attach organic appendages to a CNT but remain unused for binding metals or ligands [83, 84, 104]. The most valuable defects are those terminating with carboxylic group on the sidewall of CNTs.

These carboxylic groups can be deprotonated to afford a negative charge, and can be used to obtain an electrostatic interaction with positively charged groups such as protonated amines [83, 84, 104, 117, 118]. SMMs with positively charged ligands are available and they have been exploited to graft on surface [119, 120]. It is necessary to point out that in the case of electrostatic interaction based grafting, charged silanes, which have been used for the creation of the first CNT-based SQUID [70], cannot be used to functionalize the surface, otherwise the grafting will be lost.

Ligand exchange reaction can be used to bind a metal ion center, i.e. lanthanide, to the carboxylic group [121, 122]. This can probably yield the highest possible coupling with the CNT. However, it is not easy to achieve the exchange with considering both the charge balance as well as the steric hindrance. Additionally, the breaking of the cluster will probably lead to a change of the magnetic property of the SMM. It can be imagined that better results are expected with single paramagnetic metal ions, and some recent research shows that the single lanthanide containing molecule is able to show magnetic bistable states.

One of the important chemical properties of carboxylic groups is that they are able to form ester with hydroxyl group and to form amide with amine, which can be used to graft molecular magnets with  $OH$  or  $NH_2$  groups onto these defect sites. The interesting point of this strategy is that,

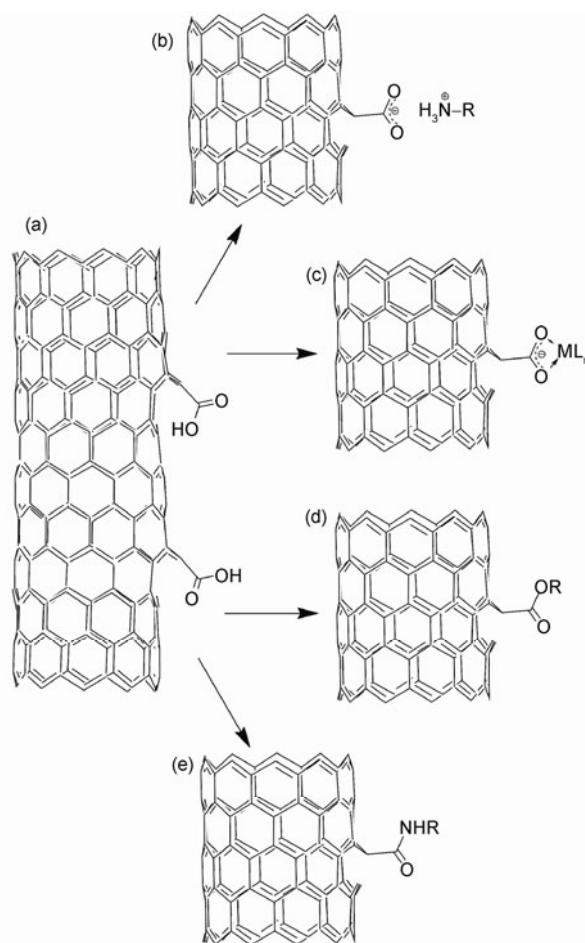


**Figure 15** Scheme of a number of useful reactions for the covalent binding of a group or a metal ion to defective sites of the CNT. (a) Carboxyl defects on a single walled CNT exploitable for the grafting of molecular magnets; (b) electrostatic interactions with positively charged molecules, i.e., protonated amines, used for anchoring nanomaterials to CNTs; (c) direct ligand exchange interactions to bind complexes of metal ions; (d) formation of an ester to covalently bind a ligand or desired molecule; (e) formation of an amide group to form a covalent bond binding a molecular magnet.

beyond forming a relatively strong coupling, by varying spacer ligand containing hydroxyl or amine group, one can tune the coupling between the molecular magnets and the CNTs, which, as aforementioned, is a rather important goal in the creation of novel molecular spintronic materials.

For both covalent and non-covalent grafting mechanism, it is of fundamental importance to control the number of grafted objects. It is then clear that new methodologies are expected for a better control than those used in solution up to now, which often involve the functionalization with a large number of nanoparticles making it much less appealing. It is also vital to point out that to graft molecular magnets onto CNTs with its structure maintenance is also difficult. This is the reason why one should choose those molecular magnets as the target molecule which is relatively stable.

Similar approaches involving graphene, although very promising, are still very limited: only the Tb double decker complexes of Figure 13 have been deposited onto grapheme [123], with scarce selectivity and not completely satisfactory control of submonolayer coverages, and the creation of SMM/carbon magnetic hybrids remains an important field of research.

## 6 Conclusions and perspectives

SMM-based molecular spintronics is an emerging field, which promises many fascinating challenges for theoreticians and experimentalists, both in Chemistry and Physics. As SMMs can modulate the response of spintronic devices, systems in which the electron flow is controlled by the quantum properties of the magnetic part can be envisaged and numerous applications can be foreseen. The quantum properties of SMMs already show appealing effects on the behavior of the devices, like negative differential conductance. In the perspective of molecular spintronic devices some SMMs do look most promising: rare-earth-based double-decker molecules, for example, are a family of isostructural SMMs with tunable anisotropy and which can produce a direct coupling with the CNTs by the overlap of the  $\pi$ -electrons of the deckers to those of the CNTs [21]. Newer systems with higher blocking temperatures [124–126] may become even more useful in the near future.

We acknowledge financial support from the Humboldt Stiftung (Sofja Kovalevskaja Prize), the German DFG (SPP 1601) and the BW Stiftung via the Kompetenznetz Funktionelle Nanostrukturen. We acknowledge Dr. M. Burghard for many stimulating discussions.

- Nitzan A, Ratner MA. Electron transport in molecular wire junctions. *Science*, 2003, 300: 1384
- Tao NJ. Electron transport in molecular junctions. *Nat Nanotechnol*, 2006, 1: 173
- Stipe BC, Rezaei MA, Ho W. Single-molecule vibrational spectroscopy and microscopy. *Science*, 1998, 280(5370): 1732–1735
- Gimzewski JK, Joachim C. Nanoscale science of single molecules using local probes. *Science*, 1999, 283(5408): 1683–1688
- Park H, Lim AKL, Alivisatos AP, Park J, McEuen PL. Fabrication of metallic electrodes with nanometer separation by electromigration. *Appl Phys Lett*, 1999, 75: 301
- Champagne AR, Pasupathy AN, Ralph DC. Mechanically adjustable and electrically gated single-molecule transistors. *Nano Lett*, 2005, 5(2): 305–308
- Osorio EA, Bjørnholm T, Lehn JM, Ruben M, van der Zant HSJ. Single-molecule transport in three-terminal devices. *J Phys: Condens Matter*, 2008, 20: 374121
- Bockrath M, Cobden DH, McEuen PL, Chopra NG, Zettl A, Thess A, Smalley RE. Single-electron transport in ropes of carbon nanotubes. *Science*, 1997, 275(5308): 1922–1925
- Tans SJ, Devoret MH, Dai HJ, Thess A, Smalley RE, Geerligs LJ, Dekker C. Individual single-wall carbon nanotubes as quantum wires. *Nature*, 1997, 386: 474
- Ponomarenko LA, Schedin F, Katsnelson MI, Yang R, Hill EW, Novoselov KS, Geim AK. Chaotic dirac billiard in graphene quantum dots. *Science*, 2008, 320: 356
- Stampfer C, Schurtenberger E, Molitor F, Guettinger J, Ihn T, Ensslin K. Tunable graphene single electron transistor. *Nano Lett*, 2008, 8: 2378
- Kastner MA. Artificial atoms. *Physics Today*, 1993, 46: 24
- Kouwenhoven LP, Austing DG, Tarucha S. Few-electron quantum dots. *Rep Prog Phys*, 2001, 64: 701
- Hanson R, Kouwenhoven LP, Petta JR, Tarucha S, Vandersypen LMK. Spins in few-electron quantum dots. *Rev Mod Phys*, 2007, 79: 1217
- Kouwenhoven LP, Marcus CM, McEuen PL, Tarucha S, Westervelt RM, Wingreen NS. *Mesoscopic Electron Transport*. In Sohn LL, Kouwenhoven LP, Schön G, Eds. Kluwer Academic Publishers, 1997
- Carlin LR. *Magnetochemistry*. Berlin, Heidelberg, New York, Tokyo: Springer-Verlag, 1986
- Kahn O. *Molecular Magnetism*. New York, Weinheim: VCH Publishers, 1993
- Miller JS. *Magnetism: Molecules to Materials*. Weinheim: WILEY-VCH, 2001–2004, 1–5
- Boyd PDW, Li QY, Vincent JB, Folting K, Chang HR, Streib WE, Huffman JC, Christou G, Hendrickson DN. Potential building-blocks for molecular ferromagnets—[Mn<sub>12</sub>O<sub>12</sub>(O<sub>2</sub>CPh)<sub>16</sub>(H<sub>2</sub>O)<sub>4</sub>] with a  $S = 14$  ground-state. *J Am Chem Soc*, 1988, 110(25): 8537–8539
- Sessoli R, Tsai HL, Schake AR, Wang SY, Vincent JB, Folting K, Gatteschi D, Christou G, Hendrickson DN. High-spin molecules—[Mn<sub>12</sub>O<sub>12</sub>(O<sub>2</sub>CR)<sub>16</sub>(H<sub>2</sub>O)<sub>4</sub>]. *J Am Chem Soc*, 1993, 115(5): 1804–1816
- Sessoli R, Gatteschi D, Caneschi A, Novak MA. Magnetic bistability in a metal-ion cluster. *Nature*, 1993, 365(6442): 141–143
- Friedman JR, Sarachik MP, Hernandez JM, Zhang XX, Tejada J, Molins E, Ziolo R. Effect of a transverse magnetic field on resonant magnetization tunneling in high-spin molecules. *J Appl Phys*, 1997, 1(8): 3978–3980
- Friedman JR, Sarachik MP, Tejada J, Ziolo R. Macroscopic measurement of resonant magnetization tunneling in high-spin molecules. *Phys Rev Lett*, 1996, 76(20): 3830–3833
- Thomas L, Lionti F, Ballou R, Gatteschi D, Sessoli R, Barbara B. Macroscopic quantum tunnelling of magnetization in a single crystal of nanomagnets. *Nature*, 1996, 383(6596): 145–147
- Barbara B, Thomas L, Lionti F, Chiorescu I, Sulpice A. Macroscopic quantum tunneling in molecular magnets. *J Mag Mag Mater*, 1999, 200(1-3): 167–181
- Wernsdorfer W. Quantum dynamics in molecular nanomagnets. *Comptes Rendus Chimie*, 2008, 11(10): 1086–1109
- Wernsdorfer W, Sessoli R. Quantum phase interference and parity effects in magnetic molecular clusters. *Science*, 1999, 284(5411): 133–135
- Jones JA. Quantum computing—Fast searches with nuclear magnetic resonance computers. *Science*, 1998, 280(5361): 229–229
- Ralph DC, Black CT, Tinkham M. Spectroscopic measurements of discrete electronic states in single metal particles. *Phys Rev Lett*, 1995, 74: 3241
- Petta JR, Ralph DC. Studies of spin-orbit scattering in noble-metal nanoparticles using energy-level tunneling spectroscopy. *Phys Rev Lett*, 2001, 87: 266801
- Johnson AT, Kouwenhoven LP, de Jong W, van der Vaart NC, Harmans CJPM, Foxon CT. Zero-dimensional states and single electron charging in quantum dots. *Phys Rev Lett*, 1992, 69: 1592
- Tarucha S, Austing DG, Honda T, van der Hage RJ, Kouwenhoven LP. Shell filling and spin effects in a few electron quantum dot. *Phys Rev Lett*, 1996, 77: 3613
- Ashoori RC. Electrons in artificial atoms. *Nature*, 1996, 379: 413
- Bockrath M, Cobden DH, McEuen PL, Chopra NG, Zettl A, Thess A, Smalley RE. Single-electron transport in ropes of carbon nanotubes. *Science*, 1997, 275: 1922
- Park J, Pasupathy AN, Goldsmith JI, Chang C, Yaish Y, Petta JR, Rinkoski M, Sethna JP, Abruna HD, McEuen PL, Ralph DC. Coulomb blockade and the Kondo effect in single-atom transistors. *Nature*, 2002, 417: 722
- Osorio EA, O'Neill K, Wegewijs MR, Stuhr-Hansen N, Paaske J, Bjørnholm T, van der Zant HSJ. Electronic excitations of a single molecule contacted in a three-terminal configuration. *Nano Lett*, 2007,

- 7: 3336
- 37 Mason N, Biercuk MJ, Marcus CM. Local gate control of a carbon nanotube double quantum dot. *Science*, 2004, 303: 655
- 38 Molitor F, Droscher S, Guttinger J, Jacobsen A, Stampfer C, Ihn T, Ensslin K. Transport through graphene double dots. *Appl Phys Lett*, 2009, 94(22): 222107
- 39 Steele GA, Gotz G, Kouwenhoven LP. Tunable few-electron double quantum dots and Klein tunnelling in ultraclean carbon nanotubes. *Nat Nanotechnol*, 2009, 4: 363
- 40 Goldhaber-Gordon D, Shtrikman H, Mahalu D, Abusch-Magder D, Meirav U, Kastner MA. Kondo effect in a single-electron transistor. *Nature*, 1998, 391(6663): 156–159
- 41 Nygard J, Cobden DH, Lindelof PE. Kondo physics in carbon nanotubes. *Nature*, 2000, 408: 342–346
- 42 Beenakker CWJ. Theory of coulomb-blockade oscillations in the conductance of a quantum dot. *Phys Rev B*, 1991, 44: 1646
- 43 van Houten H, Beenakker CWJ, Staring AAM. *Single Charge Tunneling*. In Grabert H, Devoret MH, Eds. New York: Plenum, 1992, 294
- 44 Winpenny RJP. *Single-Molecule Magnets and Related Phenomena*. In P., W. R. J., Ed. Berlin: Structure & Bonding, 2006, 122
- 45 Gatteschi D, Sessoli R, Villain J. *Molecular Nanomagnets*. New York: Oxford University Press, 2006
- 46 Lis T. Preparation, structure, and magnetic-properties of a dodecanuclear mixed-valence manganese carboxylate. *Acta Cryst B*, 1980, 36(Sep): 2042–2046
- 47 Gatteschi D, Sessoli R. Quantum tunneling of magnetization and related phenomena in molecular materials. *Angew Chem Int Ed*, 2003, 42: 268–297
- 48 Caneschi A, Gatteschi D, Sessoli R, Barra AL, Brunel LC, Guillot M. Alternating-current susceptibility, high-field magnetization, and millimeter band epr evidence for a ground  $S = 10$  state in  $[\text{Mn}_{12}\text{O}_{12}(\text{CH}_3\text{COO})_{16}(\text{H}_2\text{O})_4]\cdot 2\text{CH}_3\text{COOH}\cdot 4\text{H}_2\text{O}$ . *J Am Chem Soc*, 1991, 113(15): 5873–5874
- 49 Tasiopoulos AJ, Vinslava A, Wernsdorfer W, Abboud KA, Christou G. Giant single-molecule magnets: A  $\{\text{Mn}_{84}\}$  torus and its supramolecular nanotubes. *Angew Chem Int Ed*, 2004, 43(16): 2117–2121
- 50 Ako AM, Hewitt IJ, Mereacre V, Clerac R, Wernsdorfer W, Anson CE, Powell AK. A ferromagnetically coupled  $\text{Mn}_{19}$  aggregate with a record  $S = 83/2$  ground spin state. *Angew Chem Int Ed*, 2006, 45(30): 4926–4929
- 51 Mills DP, Moro F, McMaster J, van Slageren J, Lewis W, Blake AJ, Liddle ST. A delocalized arene-bridged diuranium single-molecule magnet. *Nat Chem*, 2011, 3(6): 454–460
- 52 Abragam A, Bleaney B. *Electron Paramagnetic Resonance of Transition Ions*. London: Oxford University Press, 1970
- 53 Kahle S, Deng Z, Malinowski N, Tonnoir C, Forment-Aliaga A, Thontasen N, Rinke G, Le D, Turkowski V, Rahman TS, Rauschenbach S, Ternes M, Kern K. The quantum magnetism of individual manganese-12-acetate molecular magnets anchored at surfaces. *Nano Lett*, 2011, 12(1): 518–521
- 54 Heersche HB, de Groot Z, Folk JA, van der Zant HSJ, Romeike C, Wegewijs MR, Zobbi L, Barreca D, Tondello E, Cornia A. Electron transport through single Mn-12 molecular magnets. *Phys Rev Lett*, 2006, 96: 206801
- 55 Kouwenhoven LP, Marcus CM, McEuen PL, Tarucha S, Westervelt RM, Wingreen NS. Electron transport in quantum dots. In *Mesoscopic Electron Transport*, Sohn LL, Kouwenhoven LP, Schön G, Eds. Kluwer, 1997, 105–214
- 56 Chakov NE, Soler M, Wernsdorfer W, Abboud KA, Christou G. Single-molecule magnets: Structural characterization, magnetic properties, and F-19 NMR spectroscopy of a Mn-12 family spanning three oxidation levels. *Inorg Chem*, 2005, 44(15): 5304–5321
- 57 Jo M-H, Grose JE, Baheti K, Deshmukh MM, Sokol JJ, Rumberger EM, Hendrickson DN, Long JR, Park H, Ralph DC. Signatures of molecular magnetism in single-molecule transport spectroscopy. *Nano Lett*, 2006, 6(9): 2014–2020
- 58 Osorio EA, Moth-Poulsen K, van der Zant HSJ, Paaske J, Hedegard P, Flensberg K, Bendix J, Bjørnholm T. Electrical manipulation of spin states in a single electrostatically gated transition-metal complex. *Nano Lett*, 2010, 10: 105
- 59 Zyazin AS, van den Berg JWG, Osorio EA, van der Zant HSJ, Konstantinidis NP, Leijnse M, Wegewijs MR, May F, Hofstetter W, Danieli C, Cornia A. Electric field controlled magnetic anisotropy in a single molecule. *Nano Lett*, 2010, 10(9): 3307–3311
- 60 Elste F, Timm C. Cotunneling and nonequilibrium magnetization in magnetic molecular monolayers. *Phys Rev B*, 2007, 75(19): 195341–195348
- 61 Timm C. Tunneling through magnetic molecules with arbitrary angle between easy axis and magnetic field. *Phys Rev B*, 2007, 76(1): 014421–014430
- 62 Romeike C, Wegewijs MR, Ruben M, Wenzel W, Schoeller H. Charge-switchable molecular magnet and spin blockade of tunneling. *Phys Rev B*, 2007, 75(6): 064404–064411
- 63 Liang WJ, Shores MP, Bockrath M, Long JR, Park H. Kondo resonance in a single-molecule transistor. *Nature*, 2002, 417(6890): 725–729
- 64 Shores MP, Sokol JJ, Long JR. Nickel(II)-molybdenum(III)-cyanide clusters: Synthesis and magnetic behavior of species incorporating  $[(\text{Me}_3\text{TACN})\text{Mo}(\text{CN})_3]$ . *J Am Chem Soc*, 2002, 124(10): 2279–2292
- 65 Romeike C, Wegewijs MR, Hofstetter W, Schoeller H. Kondo-transport spectroscopy of single molecule magnets. *Phys Rev Lett*, 2006, 97(20): 206601–206604
- 66 Romeike C, Wegewijs MR, Hofstetter W, Schoeller H. Quantum-tunneling-induced Kondo effect in single molecular magnets. *Phys Rev Lett*, 2006, 96(19): 196601–196604
- 67 Leuenberger MN, Mucciolo ER. Berry-phase oscillations of the kondo effect in single-molecule magnets. *Phys Rev Lett*, 2006, 97(12): 126601–126604
- 68 Shimada H, Ono K, Ootuka Y. Driving the single-electron device with a magnetic field (invited). *J Appl Phys*, 2003, 93(10): 8259–8264
- 69 Datta S, Marty L, Cleuziou JP, Tilmaciuc C, Soula B, Flahaut E, Wernsdorfer W. Magneto-coulomb effect in carbon nanotube quantum dots filled with magnetic nanoparticles. *Phys Rev Lett*, 2011, 107(18): 186804
- 70 Cleuziou JP, Wernsdorfer W, Bouchiat V, Ondarcuhu T, Monthieux M. Carbon nanotube superconducting quantum interference device. *Nat Nanotechnol*, 2006, 1(1): 53–59
- 71 Maurand R, Meng T, Bonet E, Florens S, Marty L, Wernsdorfer W. First-order  $0-\pi$  quantum phase transition in the kondo regime of a superconducting carbon-nanotube quantum dot. *Phys Rev X*, 2012, 2(1): 011009
- 72 Urdampilleta M, Klyatskaya S, Cleuziou JP, Ruben M, Wernsdorfer W. Supramolecular spin valves. *Nat Mater*, 2011, 10(7): 502–506
- 73 Candini A, Klyatskaya S, Ruben M, Wernsdorfer W, Affronte M. Graphene spintronic devices with molecular nanomagnets. *Nano Lett*, 2011, 11(7): 2634–2639
- 74 Steele GA, Hüttel AK, Witkamp B, Poot M, Meerwaldt HB, Kouwenhoven LP, van der Zant HSJ. Strong coupling between single-electron tunneling and nanomechanical motion. *Science*, 2009, 325: 1103
- 75 Bogani L, Santandrea F. in preparation
- 76 Bogani L, Wernsdorfer W. A perspective on combining molecular nanomagnets and carbon nanotube electronics. *Inorg Chim Acta*, 2008, 361(14–15): 3807–3819
- 77 Loiseau A, Launois P, Petit P, Roche S, Salvetat J-P. *Understanding Carbon Nanotubes: from Basics to Application, Lecture Notes in Physics Series*. Heidelberg: Springer, 2006
- 78 Rotkin SV, Subramoney S. *Applied Physics of Carbon Nanotubes: Fundamentals of Theory, Optics and Transport Devices*. Heidelberg: Springer, 2005
- 79 Dresselhaus MS, Dresselhaus G, Avouris P. *Carbon Nanotubes: Synthesis, Structure, Properties and Applications*. Heidelberg: Springer, 2001
- 80 Baughman RH, Zakhidov AA, de Heer WA. Carbon nanotubes—the route toward applications. *Science*, 2002, 297(5582): 787–792
- 81 Avouris P. Molecular electronics with carbon nanotubes. *Accounts Chem Res*, 2002, 35(12): 1026–1034

- 82 Charlier JC, Blase X, Roche S. Electronic and transport properties of nanotubes. *Rev Mod Phys*, 2007, 79(2): 677–732
- 83 Sun YP, Fu KF, Lin Y, Huang WJ. Functionalized carbon nanotubes: Properties and applications. *Accounts Chem Res*, 2002, 35(12): 1096–1104
- 84 Balasubramanian K, Burghard M. Chemically functionalized carbon nanotubes. *Small*, 2005, 1(2): 180–192
- 85 Saito R, Fujita M, Dresselhaus G, Dresselhaus MS. Electronic-structure of chiral graphene tubules. *Appl Phys Lett*, 1992, 60(18): 2204–2206
- 86 Tans SJ, Devoret MH, Dai HJ, Thess A, Smalley RE, Geerligs LJ, Dekker C. Individual single-wall carbon nanotubes as quantum wires. *Nature*, 1997, 386(6624): 474–477
- 87 Thess A, Lee R, Nikolaev P, Dai HJ, Petit P, Robert J, Xu CH, Lee YH, Kim SG, Rinzler AG, Colbert DT, Scuseria GE, Tomanek D, Fischer JE, Smalley RE. Crystalline ropes of metallic carbon nanotubes. *Science*, 1996, 273(5274): 483–487
- 88 Kane CL, Mele EJ. Size, shape, and low energy electronic structure of carbon nanotubes. *Phys Rev Lett*, 1997, 78(10): 1932–1935
- 89 Ouyang M, Huang JL, Cheung CL, Lieber CM. Energy gaps in “metallic” single-walled carbon nanotubes. *Science*, 2001, 292(5517): 702–705
- 90 Heyd R, Charlier A, McRae E. Uniaxial-stress effects on the electronic properties of carbon nanotubes. *Phys Rev B*, 1997, 55(11): 6820–6824
- 91 Minot ED, Yaish Y, Sazonova V, Park JY, Brink M, McEuen PL. Tuning carbon nanotube band gaps with strain. *Phys Rev Lett*, 2003, 90(15): 156404–156407
- 92 Yang L, Han J. Electronic structure of deformed carbon nanotubes. *Phys Rev Lett*, 2000, 85(1): 154–157
- 93 Kwon YK, Tomanek D. Electronic and structural properties of multiwall carbon nanotubes. *Phys Rev B*, 1998, 58(24): 16001–16004
- 94 Misewich JA, Martel R, Avouris P, Tsang JC, Heinze S, Tersoff J. Electrically induced optical emission from a carbon nanotube FET. *Science*, 2003, 300(5620): 783–786
- 95 Bogani L, Wernsdorfer W. Molecular spintronics using single-molecule magnets. *Nature Mater*, 2008, 7(3): 179–186
- 96 Dei A. Photomagnetic effects in polycyanometallate compounds: An intriguing future chemically based technology? *Angew Chem Int Ed*, 2005, 44(8): 1160–1163
- 97 Carbonera C, Dei A, Letard JF, Sangregorio C, Sorace L. Thermally and light-induced valence tautomeric transition in a dinuclear cobalt-tetraoxolene complex. *Angew Chem Int Ed*, 2004, 43(24): 3136–3138
- 98 Gutlich P, Dei A. Valence tautomeric interconversion in transition metal 1,2-benzoquinone complexes. *Angew Chem Int Ed*, 1997, 36(24): 2734–2736
- 99 Adams DM, Dei A, Rheingold AL, Hendrickson DN. Controlling valence tautomerism of cobalt complexes containing the benzosemiquinone anion as ligand. *Angew Chem Int Ed*, 1993, 32(6): 880–882
- 100 Giraud R, Wernsdorfer W, Tkachuk AM, Mailly D, Barbara B. Nuclear spin driven quantum relaxation in  $\text{LiY}_{0.998}\text{Ho}_{0.002}\text{F}_4$ . *Phys Rev Lett*, 2001, 87(5): 057203
- 101 Ishikawa N, Sugita M, Wernsdorfer W. Quantum tunneling of magnetization in lanthanide single-molecule magnets: Bis(phthalocyaninato)terbium and bis(phthalocyaninato)dysprosium anions. *Angew Chem Int Ed*, 2005, 44(19): 2931–2935
- 102 Ishikawa N, Sugita M, Ishikawa T, Koshihara S, Kaizu Y. Lanthanide double-decker complexes functioning as magnets at the single-molecular level. *J Am Chem Soc*, 2003, 125(29): 8694–8695
- 103 Ishikawa N, Sugita M, Wernsdorfer W. Nuclear spin driven quantum tunneling of magnetization in a new lanthanide single-molecule magnet: Bis(phthalocyaninato)holmium anion. *J Am Chem Soc*, 2005, 127(11): 3650–3651
- 104 Britz DA, Khlobystov AN. Noncovalent interactions of molecules with single walled carbon nanotubes. *Chem Soc Rev*, 2006, 35(7): 637–659
- 105 Liu Z, Sun XM, Nakayama-Ratchford N, Dai HJ. Supramolecular chemistry on water-soluble carbon nanotubes for drug loading and delivery. *ACS Nano*, 2007, 1(1): 50–56
- 106 Hirsch A. Functionalization of single-walled carbon nanotubes. *Angew Chem Int Ed*, 2002, 41(11): 1853–1859
- 107 Charlier JC. Defects in carbon nanotubes. *Acc Chem Res*, 2002, 35(12): 1063–1069
- 108 Kim W, Javey A, Vermesh O, Wang O, Li YM, Dai HJ. Hysteresis caused by water molecules in carbon nanotube field-effect transistors. *Nano Lett*, 2003, 3(2): 193–198
- 109 Bogani L, Danieli C, Biavardi E, Bendiab N, Barra AL, Dalcanale E, Wernsdorfer W, Cornia A. Single-molecule-magnet carbon-nanotube hybrids. *Angew Chem Int Ed*, 2009, 48(4): 746–750
- 110 Bogani L, Maurand R, Marty L, Sangregorio C, Altavilla C, Wernsdorfer W. Effect of sequential grafting of magnetic nanoparticles onto metallic and semiconducting carbon-nanotube devices: towards self-assembled multi-dots. *J Mater Chem*, 2010, 20(11): 2099–2107
- 111 Bogani L, Caneschi A, Fedi M, Gatteschi D, Massi M, Novak MA, Pini MG, Rettori A, Sessoli R, Vindigni A. Finite-size effects in single chain magnets: An experimental and theoretical study. *Phys Rev Lett*, 2004, 92(20): 207204–207207
- 112 Bogani L, Sessoli R, Pini MG, Rettori A, Novak MA, Rosa P, Massi M, Fedi ME, Giuntini L, Caneschi A, Gatteschi D. Finite-size effects on the static properties of a single-chain magnet. *Phys Rev B*, 2005, 72(6): 064406–064415
- 113 Kyatskaya S, Galan-Mascaros JR, Bogani L, Hennrich F, Kappes M, Wernsdorfer W, Ruben M. Anchoring of rare-earth-based single-molecule magnets on single-walled carbon nanotubes. *J Am Chem Soc*, 2009, 131(42): 15143–15151
- 114 Accorsi G, Armaroli N, Parisini A, Meneghetti M, Marega R, Prato M, Bonifazi D. Wet adsorption of a luminescent Eu-III complex on carbon nanotubes sidewalls. *Adv Funct Mater*, 2007, 17(15): 2975–2982
- 115 Raghuvver MS, Kumar A, Frederick MJ, Louie GP, Ganesan PG, Ramanath G. Site-selective functionalization of carbon nanotubes. *Adv Mater*, 2006, 18(5): 547–552
- 116 Koshio A, Yudasaka M, Zhang M, Iijima S. A simple way to chemically react single-wall carbon nanotubes with organic materials using ultrasonication. *Nano Lett*, 2001, 1(7): 361–363
- 117 Wilgoose GG, Banks CE, Compton RG. Metal nanoparticles and related materials supported on carbon nanotubes: Methods and applications. *Small*, 2006, 2(2): 182–193
- 118 Jiang KY, Eitan A, Schadler LS, Ajayan PM, Siegel RW, Grobert N, Mayne M, Reyes-Reyes M, Terrones H, Terrones M. Selective attachment of gold nanoparticles to nitrogen-doped carbon nanotubes. *Nano Lett*, 2003, 3(3): 275–277
- 119 Coronado E, Forment-Aliaga A, Romero FM, Corradini V, Biagi R, De Renzi V, Gambardella A, del Pennino U. Isolated Mn-12 single-molecule magnets grafted on gold surfaces via electrostatic interactions. *Inorg Chem*, 2005, 44(22): 7693–7695
- 120 Coronado E, Forment-Aliaga A, Gaita-Arino A, Gimenez-Saiz C, Romero FM, Wernsdorfer W. Polycationic  $\text{Mn}_{12}$  single-molecule magnets as electron reservoirs with  $S > 10$  ground states. *Angew Chem Int Ed*, 2004, 43(45): 6152–6156
- 121 Banerjee S, Wong SS. Structural characterization, optical properties, and improved solubility of carbon nanotubes functionalized with Wilkinson's catalyst. *J Am Chem Soc*, 2002, 124(30): 8940–8948
- 122 Banerjee S, Wong SS. Functionalization of carbon nanotubes with a metal-containing molecular complex. *Nano Lett*, 2002, 2(1): 49–53
- 123 Lopes M, Candini A, Urdampilleta M, Reserbat-Plantey A, Bellini V, Klyatskaya S, Marty Lt, Ruben M, Affronte M, Wernsdorfer W, Bendiab N. Surface-enhanced raman signal for terbium single-molecule magnets grafted on graphene. *ACS Nano*, 2010, 4(12): 7531–7537
- 124 Jiang SD, Wang BW, Su G, Wang ZM, Gao S. A mononuclear dysprosium complex featuring single-molecule-magnet behavior. *Angew Chem Int Ed*, 2010, 49(41): 7448–7451
- 125 Jiang SD, Wang BW, Sun HL, Wang ZM, Gao S. An organometallic single-ion magnet. *J Am Chem Soc*, 2011, 133(13): 4730–4733
- 126 Jiang SD, Liu SS, Zhou LN, Wang BW, Wang ZM, Gao S. Series of lanthanide organometallic single-ion magnets. *Inorg Chem*, 2012, 51(5): 3079–3087